Inorg. Chem. **2004**, *43*, 7359–7368

Mononuclear and Binuclear Wirelike Ruthenium(II) Complexes with Oligo-diethynyl-thiophene Bridged Back-to-Back Terpyridine Ligands: Synthesis and Electrochemical and Photophysical Properties

Andrea Barbieri,*,† Barbara Ventura,† Francesco Barigelletti,† Antoinette De Nicola,‡ Manuel Quesada,‡ and Raymond Ziessel*,‡

Istituto per la Sintesi Organica e la Fotoreattività, Consiglio Nazionale delle Ricerche (ISOF-CNR), Via P. Gobetti 101, 40129 Bologna, Italy, and Laboratoire de Chimie Moléculaire, Ecole de Chimie, Polymères, Matériaux (ECPM), Université Louis Pasteur (ULP), 25 rue Becquerel, 67087 Strasbourg Cedex 02, France

Received May 28, 2004

The syntheses, structural features, electrochemical behavior, absorption spectra, and photophysical properties of five mononuclear complexes [(terpy)Ru(terpy-DEDBT$_n$-terpy)]$^{2+}$, **RuT$_n$**, and five binuclear complexes [(terpy)Ru-(terpy-DEDBT$_n$-terpy)Ru(terpy)]$^{4+}$, **RuT$_n$Ru**, are reported, where n varies from 1 to 5 so that the metal–metal distance is estimated to be 42 Å for the largest binuclear complex, **RuT$_5$Ru** (terpy is 2,2′:6′,2″-terpyridine and DEDBT is 2,5-diethynyl-3,4-dibutylthiophene). The metal-centered oxidation potentials for the mononuclear and binuclear species are slightly more positive than for the reference [Ru(terpy)$_2$]$^{2+}$ complex, owing to the withdrawing nature of the back-to-back terpyridine ligands incorporating the repeat diethynyl-thiophene units. Comparison of the reduction potentials for the mononuclear and binuclear complexes reveals that the reduction steps are localized either at the terpy fragments of the **T$_n$** ligands or at the terpy peripheral ligands. The spectroscopic results (absorption spectra at room temperature, luminescence spectra and lifetimes at room temperature and at 77 K) in acetonitrile solvent are consistent with the establishment of electronic delocalization within the oligomeric diethynyl-thiophene fragments (DEDBT$_n$) of the **T$_n$** ligands; however, the results also indicate that the terpy units of these ligands and the DEDBT$_n$ fragments are not strongly coupled. Both at room temperature and at 77 K, the ^{3}metal-to-ligand charge-transfer luminescence of **RuT$_n$** and **RuT$_n$Ru** complexes is strongly depressed in the larger species with respect to what happens for $n \leq 2$ (where the luminescence quantum yield is $\phi \approx 10^{-4}$); this is discussed in terms of the possible intervention of triplet levels localized at the oligothiophene DEDBT$_n$ fragments.

Introduction

The design, synthesis, and characterization of polypyridine complexes of Ru(II) is an area of widespread interest that has found applications in energy conversion systems such as dye-sensitized solar cells[1−4] and electroluminescent devices.[5−8] These complexes possess valuable electrochemical, photophysical, and photochemical properties,[9,10] and derived polynuclear complexes are topologically interesting species including rods, wires, helicates, and dendrimers scaffolds.[11−18]

* Authors to whom correspondence should be addressed. E-mail: barbieri@isof.cnr.it; ziessel@chimie.u-strasbg.fr.
† Consiglio Nazionale delle Ricerche.
‡ Université Louis Pasteur.

(1) Hagfeldt, A.; Grätzel, M. *Acc. Chem. Res.* **2000**, *33*, 269.
(2) Bignozzi, C. A.; Argazzi, R.; Kleverlaan, C. J. *Chem. Soc. Rev.* **2000**, *29*, 87.
(3) Wang, P.; Zakeeruddin, S. M.; Moser, J. E.; Nazeeruddin, M. K.; Sekiguchi, T.; Grätzel, M. *Nat. Mater.* **2003**, *2*, 402.
(4) Islam, A.; Sugihara, H.; Arakawa, H. *J. Photochem. Photobiol., A* **2003**, *158*, 131.
(5) Slinker, J.; Bernards, D.; Houston, P. L.; Abruna, H. D.; Bernhard, S.; Malliaras, G. G. *Chem. Commun.* **2003**, 2392.
(6) Kalyuzhny, G.; Buda, M.; McNeill, J.; Barbara, P.; Bard, A. J. *J. Am. Chem. Soc.* **2003**, *125*, 6272.
(7) Rudmann, H.; Shimada, S.; Rubner, M. F. *J. Am. Chem. Soc.* **2002**, *124*, 4918.
(8) Welter, S.; Brunner, K.; Hofstraat, J. W.; De Cola, L. *Nature* **2003**, *421*, 54.
(9) Juris, A.; Balzani, V.; Barigelletti, F.; Campagna, S.; Belser, P.; von Zelewsky, A. *Coord. Chem. Rev.* **1988**, *84*, 85.
(10) Sauvage, J. P.; Collin, J. P.; Chambron, J. C.; Guillerez, S.; Coudret, C.; Balzani, V.; Barigelletti, F.; De Cola, L.; Flamigni, L. *Chem. Rev.* **1994**, *94*, 993.
(11) Constable, E. C. *Prog. Inorg. Chem.* **1994**, *42*, 67.
(12) Balzani, V.; Juris, A.; Venturi, M.; Campagna, S.; Serroni, S. *Chem. Rev.* **1996**, *96*, 759.

10.1021/ic0493043 CCC: $27.50
Published on Web 10/14/2004

The design of novel polynuclear species in view of applications is based on a careful choice of the coordinated ligands and the bridging units; a close scrutiny of implied requirements is needed. These include the chemical accessibility of the components and the envisaged versatility along synthetic routes, the capability of the ligands to confer desired structural properties, the thermal and photochemical stability of the species, and their electrochemical and spectroscopic properties.

From a geometrical viewpoint, suitable building blocks for the construction of topographically linear polynuclear species are based on the $[Ru(terpy)_2]^{2+}$ motifs (terpy is 2,2′:6′,2″-terpyridine).[10,11,14] The luminescence properties of $[Ru(terpy)_2]^{2+}$ salts are, however, very poor ($\phi < 10^{-5}$, $\tau <$ 1 ns),[10,14] which has stimulated several lines of activity aimed at achieving significant luminescence improvements. A common approach has been that of developing suitable functionalities starting from the 4′ position of a coordinated terpy. In general terms, nicely performing systems are made available by employing groups able to extend the electronic conjugation.[19,20] Among these, ligands of the terpy-ethynyl type have proven very useful and have provided a rich library of highly luminescent complexes derived from the basic Ru(II)-terpy-type module.[14,21,22] Quite recently, complexes containing units such as thiophene, polythiophenes, and ethynyl-thiophene have also been employed to develop linear arrays of luminescent complexes of Ru(II) and Os(II).[23−27] Thus, new wirelike species become available that incorporate thiophene-containing π-conjugated fragments; the study of their photophysical properties is of relevance, given the importance of thiophene and oligomeric polythiophenes as electro- and photoactive conjugated materials.[28−37]

In the present paper, we report on the preparation and characterization, the electrochemical behavior, and the photophysical properties of a series of linearly arranged metal complexes, $[(terpy)Ru(terpy\text{-}DEDBT_n\text{-}terpy)]^{2+}$, **RuT*n***, and $[(terpy)Ru(terpy\text{-}DEDBT_n\text{-}terpy)Ru(terpy)]^{4+}$, **RuT*n*Ru**, featuring Ru(II)−terpy chromophores connected to π-conjugated 2,5-diethynyl-3,4-dibutylthiophene oligomeric fragments, terpy−$DEDBT_n$−terpy (**T*n***), with $n = 1$, 2, 3, 4, and 5; the preparation and characterization of these ligands was recently reported.[38] Chart 1 shows schematic structures of the **T*n*** ligands and of the complexes. In the binuclear complexes **RuT*n*Ru**, the connecting **T*n*** ligands provide a structurally rigid linkage between the two chromophoric centers, with estimated intermetal separations of 18.5, 24.9, 30.7, 36.1, and 41.6 Å for $n = 1$, 2, 3, 4, and 5, respectively, (from ZINDO/1 semiempirical self-consistent field (SCF) calculations according to Hyperchem 7.5); Chart 2 illustrates the results for the largest species investigated, **RuT5Ru**. The electrochemical and spectroscopic properties of the examined mononuclear and binuclear complexes allow us to address the electronic properties of the connecting **T*n*** ligands, incorporating the $DEDBT_n$ oligomers. With respect to the parent $[Ru(terpy)_2]^{2+}$ complex,[10,14] the complexes studied here feature better luminescence properties in acetonitrile solvent, $\tau = 100-160$ ns and $\phi \approx 10^{-4}$ for $n \leq 2$.

Chart 1. Investigated Ligands and Derived Mono- and Binuclear Ruthenium Complexes $n = 1-5$

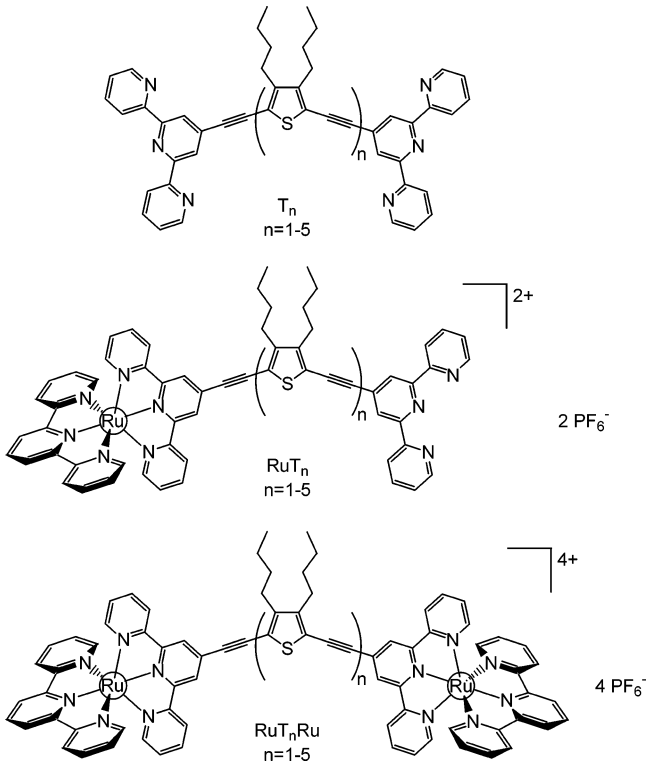

(13) Keene, F. R. *Coord. Chem. Rev.* **1997**, *166*, 121.
(14) Harriman, A.; Ziessel, R. *Chem. Commun.* **1996**, 1707.
(15) Balzani, V.; Campagna, S.; Denti, G.; Juris, A.; Serroni, S.; Venturi, M. *Acc. Chem. Res.* **1998**, *31*, 26.
(16) Constable, E. C. *Chem. Commun.* **1997**, 1073.
(17) De Cola, L.; Belser, P. *Coord. Chem. Rev.* **1998**, *177*, 301.
(18) Barigelletti, F.; Flamigni, L. *Chem. Soc. Rev.* **2000**, *29*, 1.
(19) El-ghayoury, A.; Harriman, A.; Khatyr, A.; Ziessel, R. *J. Phys. Chem. A* **2000**, *104*, 1512.
(20) Passalacqua, R.; Loiseau, F.; Campagna, S.; Fang, Y. Q.; Hanan, G. S. *Angew. Chem., Int. Ed.* **2003**, *42*, 1608.
(21) Grosshenny, V.; Ziessel, R. *J. Organomet. Chem.* **1993**, *453*, C19.
(22) Harriman, A.; Mayeux, A.; De Nicola, A.; Ziessel, R. *Phys. Chem. Chem. Phys.* **2002**, *4*, 2229.
(23) Encinas, S.; Flamigni, L.; Barigelletti, F.; Constable, E. C.; Housecroft, C. E.; Schofield, E. R.; Figgemeier, E.; Fenske, D.; Neuburger, M.; Vos, J. G.; Zehnder, M. *Chem.−Eur. J.* **2002**, *8*, 137.
(24) Liu, Y.; De Nicola, A.; Reiff, O.; Ziessel, R.; Schanze, F. S. *J. Phys. Chem. A* **2003**, *107*, 3476.
(25) De Nicola, A.; Liu, Y.; Schanze, K. S.; Ziessel, R. *Chem. Commun.* **2003**, 288.
(26) De Nicola, A.; Ringenbach, C.; Ziessel, R. *Tetrahedron Lett.* **2003**, *44*, 183.
(27) Walters, K. A.; Trouillet, L.; Guillerez, S.; Schanze, K. S. *Inorg. Chem.* **2000**, *39*, 5496.
(28) Roncali, J. *Chem. Rev.* **1997**, *97*, 173.
(29) Roncali, J. *Acc. Chem. Res.* **2000**, *33*, 147.
(30) Apperloo, J. J.; Janssen, R. A. J.; Malenfant, P. R. L.; Frechet, J. M. J. *J. Am. Chem. Soc.* **2001**, *123*, 6916.
(31) Pappenfus, T. M.; Mann, K. R. *Inorg. Chem.* **2001**, *40*, 6301.
(32) Casado, J.; Miller, L. L.; Mann, K. R.; Pappenfus, T. M.; Higuchi, H.; Orti, E.; Milian, B.; Pou-Amerigo, R.; Hernandez, V.; Navarrete, J. T. L. *J. Am. Chem. Soc.* **2002**, *124*, 12380.
(33) Hjelm, J.; Constable, E. C.; Figgemeier, E.; Hagfeldt, A.; Handel, R.; Housecroft, C. E.; Mukhtar, E.; Schofield, E. *Chem. Commun.* **2002**, 284.
(34) Otsubo, T.; Aso, Y.; Takimiya, K. *J. Mater. Chem.* **2002**, *12*, 2565.
(35) Becker, R. S.; deMelo, J. S.; Macanita, A. L.; Elisei, F. *J. Phys. Chem.* **1996**, *100*, 18683.
(36) Groenendaal, B. L.; Jonas, F.; Freitag, D.; Pielartzik, H.; Reynolds, J. R. *Adv. Mater.* **2000**, *12*, 481.
(37) Ng, S. C.; Ong, T. T.; Chan, H. S. O. *J. Mater. Chem.* **1998**, *8*, 2663.
(38) Ringenbach, C.; De Nicola, A.; Ziessel, R. *J. Org. Chem.* **2003**, *68*, 4708.

Chart 2. Molecular Structure of **RuT$_5$Ru** According to ZINDO/1 Semiempirical SCF Calculations (Results from Hyperchem 7.5)

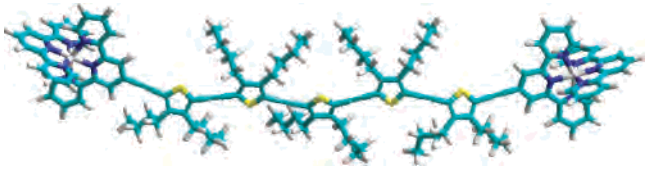

Experimental Section

General Methods. The 200.1 (^{1}H) NMR (Brücker AC 200) spectra were recorded at room temperature using perdeuterated solvent as an internal standard, δ (H) in ppm relative to residual protiated solvent in acetone-d_6 (2.05). Fast-atom bombardment (FAB, in a positive mode) analyses were performed using a ZAB-HF-VB analytical apparatus and *m*-nitrobenzyl alcohol (*m*-NBA) as the matrix. Elemental analyses (C, H, N) were performed using an elemental analyzer (Thermo Electron Flash EA 1112, accuracy better than 0.3%). Structural features of the mono- and binuclear complexes were estimated from ZINDO/1 semiempirical SCF calculations performed with Hyperchem 7.5 (where constant orbital exponents are used for all of the available elements, including second-row transition metals, and both overlapping factors ($\sigma-\sigma$ and $\pi-\pi$) were set to 1).

Electrochemical Measurements. Electrochemical studies employed cyclic voltammetry with a conventional three-electrode system using a BAS CV-50W voltammetric analyzer equipped with a Pt microdisk (2 mm^2) working electrode and a platinum wire counter electrode. Ferrocene was used as an internal standard and was calibrated against a saturated calomel reference electrode (SCE) separated from the electrolysis cell by a glass frit presoaked with electrolyte solution. Solutions contained the electroactive substrate (ca. 1×10^{-4} to 1×10^{-3} M) in deoxygenated and anhydrous acetonitrile with tetra-*n*-butylammonium hexafluorophosphate (0.1 M) as the supporting electrolyte. For the mononuclear complexes, the use of a very low concentration avoided the strong adsorption of the complexes to the Pt electrode and the occurrence of stripping peaks. The quoted half-wave potentials were reproducible within $\pm$10 mV.

Optical Spectroscopy. Absorption spectra of dilute dichloromethane (for the ligands) and acetonitrile (for the complexes) solutions (2×10^{-5} M) were obtained with a Perkin-Elmer Lambda 45 UV/vis spectrometer. Luminescence spectra were obtained with a Spex Fluorolog II spectrofluorimeter, equipped with a Hamamatsu R928 phototube. Air-equilibrated and freeze−pump−thaw degassed sample solutions were excited at the indicated wavelength, and dilution was adjusted to obtain absorbance values $\leq$0.15. Although uncorrected luminescence band maxima are used throughout the text, corrected spectra were employed for the determination of the luminescence quantum yields. The correction procedure is based on the use of software that takes care of the wavelength-dependent phototube response. From the wavelength-integrated area of the corrected luminescence spectra, we obtained luminescence quantum yields ϕ for the samples with reference to [Ru(bpy)$_3$]Cl$_2$ (r, ϕ_r = 0.028 in air-equilibrated water[39]) and by using eq 1,[40]

$$\frac{\phi}{\phi_r} = \frac{\mathrm{Abs}_r\, n^2\, (\mathrm{area})}{\mathrm{Abs}\, n_r^2\, (\mathrm{area})_r} \qquad (1)$$

where Abs and *n* are absorbance values and refractive index of the solvent, respectively. Band maxima and relative luminescence intensities were affected by uncertainties of 2 nm and 20%, respectively. Luminescence lifetimes were obtained by using an IBH 5000F single-photon counting spectrometer equipped with entry and exit monochromators; excitation was performed either with a nitrogen-filled thyratron-gated lamp (λ_{exc} 337 or 358 nm) or by using 375- and 465-nm nanoLED sources, and observations were made in the correspondence of the emission peak. Single-exponential decays were found in all cases. The uncertainty in the lifetime values was within 8%.

Materials. The back-to-back terpyridine ligands[38] and the *cis*-[Ru(terpy)(DMSO)Cl$_2$][21] precursor were prepared according to literature procedures.

General Procedure for the Synthesis of the Mononuclear RuT$_n$ and Binuclear RuT$_n$Ru Complexes. In a Schlenk flask, a stirred solution of 2 equiv (for **T$_1$** to **T$_3$** derivatives) or 2.5 equiv (for **T$_4$** and **T$_5$** derivatives) of *cis*-[Ru(terpy)(DMSO)Cl$_2$] and 4.2 equiv (for **T$_1$** to **T$_3$** derivatives) or 5.2 equiv (for **T$_4$** and **T$_5$** derivatives) of AgBF$_4$ in an argon-degassed methanol solution (20 mL) was held at 80 °C for 6 h. After being cooled to room temperature, the deep-red solution was filtered over cotton wool and transferred via cannula to an argon-degassed dichloromethane solution containing 1 equiv of the corresponding ditopic ligands (**T$_n$**). During heating at 80 °C, the deep-red solution turned red-orange showing slow ruthenium complexation. After the complete consumption of the starting material (determined by TLC), an aqueous solution (5 equiv) of KPF$_6$ was added; the organic solvent was then removed under vacuum, and the precipitates were washed by centrifugation with water until the solution was colorless. The target complexes were purified by chromatography on alumina eluting with dichloromethane using a gradient of methanol. The pure red complexes were obtained by double recrystallization in acetone/hexane.

RuT$_1$ and RuT$_1$Ru were prepared following the general procedure from *cis*-[Ru(terpy)(DMSO)Cl$_2$] (0.038 g, 0.079 mmol), AgBF$_4$ (0.032 g, 0.166 mmol), and **T$_1$** (0.028 g, 0.040 mmol) for 20 h; chromatography was performed by eluting first with dichloromethane until dichloromethane/methanol (v/v 95/5) to afford after recrystallization 16 mg (38%) of **RuT$_1$** and 20 mg (36%) of **RuT$_1$Ru**.

RuT$_1$. ^{1}H NMR (200 MHz, acetone-d_6): δ 9.23 (s, 2H), 9.11 (m, 2H), 8.77 (m, 11H), 8.10 (6H), 7.80 (m, 4H), 7.54 (m, 2H), 7.37 (m, 4H), thiophene alkyl chain protons are overlapping with residual solvent. UV−vis (CH$_3$CN) λ/nm (ϵ/M^{-1} cm^{-1}): 498 (43 800), 388 (43 200), 307 (71 600), 272 (67 100). FAB$^+$ *m*/*z* (nature of the peak, relative intensity): 1186.3 ([M-PF$_6$]$^+$, 100), 520.5 ([M-2PF$_6$]$^{2+}$, 15). Anal. Calcd for $C_{61}H_{49}N_9SRuP_2F_{12}$ (M_w = 1331.16): C, 55.04; H, 3.71; N, 9.47. Found: C, 54.79; H, 3.45; N, 9.23.

RuT$_1$Ru. ^{1}H NMR (200 MHz, acetone-d_6): δ 9.23 (s, 4H), 9.12 (d, J = 8.1 Hz, 4H), 8.88 (m, 8H), 8.63 (t, J = 8.1 Hz, 2H), 8.10 (m, 8H), 7.80 (m, 8H), 7.37 (m, 8H) thiophene alkyl chain protons are overlapping with residual solvent; UV−vis (CH$_3$CN) λ/nm (ϵ/M^{-1} cm^{-1}): 512 (79 700), 395 (40 100), 307 (117 400), 272 (90 600). FAB$^+$ *m*/*z* (nature of the peak, relative intensity): 1811.3 ([M-PF$_6$]$^+$, 100), 833.2 ([M-2PF$_6$]$^{2+}$, 15). Anal. Calcd for $C_{76}H_{60}N_{12}SRu_2P_4F_{24}\cdot CH_3OH$ (M_w = 1955.43 + 32.04): C, 46.53; H, 3.25; N 8.46. Found: C, 46.29; H, 3.07; N, 8.19.

RuT$_2$ and RuT$_2$Ru were prepared following the general procedure from *cis*-[Ru(terpy)(DMSO)Cl$_2$] (0.065 g, 0.134 mmol), AgBF$_4$ (0.055 g, 0.282 mmol), and **T$_2$** (0.062 g, 0.067 mmol) for 48 h; chromatography was performed by eluting first with dichloromethane until dichloromethane/methanol (v/v 95/5)

(39) Nakamaru, K. *Bull. Chem. Soc. Jpn.* **1982**, *55*, 2967.
(40) Demas, J. N.; Crosby, G. A. *J. Phys. Chem.* **1971**, *75*, 991.

to afford after recrystallization 27 mg (14%) of **RuT$_2$** and 18 mg (8%) of **RuT$_2$Ru**.

RuT$_2$. ^{1}H NMR (200 MHz, acetone-d_6): δ 9.20 (s, 2H), 9.11 (m, 2H), 8.75 (m, 11H), 8.08 (6H), 7.80 (m, 4H), 7.52 (m, 2H), 7.37 (m, 4H), 1.61 (m, 16H), 1.13 (m, 12H); UV−vis (CH_3CN) λ/nm (ϵ/M^{-1} cm^{-1}): 503 (52 200), 422 (44 200), 307 (71 200), 273 (67 400). FAB$^+$ *m*/*z* (nature of the peak, relative intensity): 1404.2 ([M-PF$_6$]$^+$, 100), 629.5 ([M-2PF$_6$]$^{2+}$, 15). Anal. Calcd for $C_{75}H_{67}N_9S_2RuP_2F_{12}$ (M_w = 1549.32): C, 58.13; H, 4.36; N, 8.13. Found: C, 57.87; H, 4.04; N, 7.94.

RuT$_2$Ru. ^{1}H NMR (200 MHz, acetone-d_6): δ 9.20 (s, 4H), 9.12 (d, J = 8.2 Hz, 4H), 8.87 (m, 8H), 8.62 (t, J = 8.2 Hz, 2H), 8.10 (m, 8H), 7.79 (m, 8H), 7.36 (m, 8H), 1.66 (m, 16H), 1.07 (m, 12H). UV−vis (CH_3CN) λ/nm (ϵ/M^{-1} cm^{-1}): 511 (92 300), 430 (46 900), 307 (116 900), 272 (90 800). FAB$^+$ *m*/*z* (nature of the peak, relative intensity): 2029.2 ([M-PF$_6$]$^+$, 100), 942.1 ([M-2PF$_6$]$^{2+}$, 15). Anal. Calcd for $C_{90}H_{78}N_{12}S_2Ru_2P_4F_{24}\cdot CH_3OH$ (M_w = 2173.79 + 32.04): C, 49.55; H, 3.75; N, 7.62. Found: C, 49.21; H, 3.44; N, 7.45.

RuT$_3$ and RuT$_3$Ru were prepared following the general procedure from *cis*-[Ru(terpy)(DMSO)Cl$_2$] (0.095 g, 0.196 mmol), $AgBF_4$ (0.080 g, 0.413 mmol), and **T$_3$** (0.110 g, 0.096 mmol) for 48 h; chromatography was performed by eluting first with dichloromethane until dichloromethane/methanol (v/v 85/15) to afford after recrystallization 49 mg (35%) of **RuT$_3$** and 21 mg (11%) of **RuT$_3$Ru**.

RuT$_3$. ^{1}H NMR (200 MHz, acetone-d_6): δ 9.20 (s, 2H), 9.12 (m, 2H), 8.75 (m, 11H), 8.07 (6H), 7.80 (m, 4H), 7.50 (m, 2H), 7.37 (m, 4H), 1.63 (m, 24H), 1.03 (m, 18H). UV−vis (CH_3CN) λ/nm (ϵ/M^{-1} cm^{-1}): 505 (53 700), 433 (59 800), 307 (71 600), 272 (67 000). FAB$^+$ *m*/*z* (nature of the peak, relative intensity): 1622.1 ([M-PF$_6$]$^+$, 100), 738.6 ([M-2PF$_6$]$^{2+}$, 25). Anal. Calcd for $C_{89}H_{85}N_9S_3RuP_2F_{12}$ (M_w = 1767.88): C, 58.13; H, 4.36; N, 8.13. Found: C, 57.88; H, 4.23; N, 7.94.

RuT$_3$Ru. ^{1}H NMR (200 MHz, acetone-d_6): δ 9.20 (s, 4H), 9.12 (d, J = 8.1 Hz, 4H), 8.87 (m, 8H), 8.63 (t, J = 8.1 Hz, 2H), 8.10 (m, 8H), 7.79 (m, 8H), 7.36 (m, 8H), 1.63 (m, 24H), 1.04 (m, 18H). UV−vis (CH_3CN) λ/nm (ϵ/M^{-1} cm^{-1}): 509 (100 200), 444 (58 100), 309 (116 000), 271 (91 400). FAB$^+$ *m*/*z* (nature of the peak, relative intensity): 2247.1 ([M-PF$_6$]$^+$, 100), 1051.2 ([M-2PF$_6$]$^{2+}$, <5). Anal. Calcd for $C_{104}H_{96}N_{12}S_3Ru_2P_4F_{24}\cdot CH_3OH$ (M_w = 2424.19 + 32.04): C, 52.02; H, 4.16; N, 6.93. Found: C, 51.79; H, 4.01; N, 6.66.

RuT$_4$ and RuT$_4$Ru were prepared following the general procedure from *cis*-[Ru(terpy)(DMSO)Cl$_2$] (0.053 g, 0.110 mmol), $AgBF_4$ (0.045 g, 0.229 mmol), and **T$_4$** (0.060 g, 0.044 mmol) for 48 h; chromatography was performed by eluting first with dichloromethane until dichloromethane/methanol (v/v 95/5) to afford after recrystallization 30 mg (40%) of **RuT$_4$** and 21 mg (24%) of **RuT$_4$Ru**.

RuT$_4$. ^{1}H NMR (200 MHz, acetone-d_6): δ 9.20 (s, 2H), 9.11 (m, 2H), 8.77 (m, 11H), 8.08 (6H), 7.79 (m, 4H), 7.50 (m, 2H), 7.36 (m, 6H), 1.62 (m, 32H), 1.03 (m, 24H). UV−vis (CH_3CN) λ/nm (ϵ/M^{-1} cm^{-1}): 505 (53 700), 433 (59 800), 307 (71 600), 272 (67 000). FAB$^+$ *m*/*z* (nature of the peak, relative intensity): 1840.2 ([M-PF$_6$]$^+$, 100), 847.6 ([M-2PF$_6$]$^{2+}$, 10). Anal. Calcd for $C_{103}H_{103}N_9S_4RuP_2F_{12}$ (M_w = 1986.24): C, 62.28; H, 5.23; N, 6.35. Found: C, 61.97; H, 4.87; N, 6.26.

RuT$_4$Ru. ^{1}H NMR (200 MHz, acetone-d_6): δ 9.20 (s, 4H), 9.11 (d, J = 8.0 Hz, 4H), 8.89 (m, 8H), 8.62 (t, J = 8.0 Hz, 2H), 8.09 (m, 8H), 7.79 (m, 8H), 7.36 (m, 8H), 1.69 (m, 32H), 1.03 (m, 24H). UV−vis (CH_3CN) λ/nm (ϵ/M^{-1} cm^{-1}): 507 (107 800), 444 (72 100), 309 (115 900), 272 (93 500). FAB$^+$ *m*/*z* (nature of the peak, relative intensity): 2465.2 ([M-PF$_6$]$^+$, 100), 1160.1 ([M-2PF$_6$]$^{2+}$, 20). Anal. Calcd for $C_{118}H_{114}N_{12}S_4Ru_2P_4F_{24}\cdot CH_3OH$ (M_w = 2610.51 + 32.04): C, 54.09; H, 4.50; N, 6.36. Found: C, 53.78; H, 4.24; N, 6.18.

RuT$_5$ and RuT$_5$Ru were prepared following the general procedure from *cis*-[Ru(terpy)(DMSO)Cl$_2$] (0.050 g, 0.104 mmol), $AgBF_4$ (0.042 g, 0.216 mmol) in 29 mL of methanol, and **T$_5$** (0.063 g, 0.040 mmol) for 6 days; chromatography was performed by eluting first with dichloromethane until dichloromethane/methanol (v/v 95/5) to afford after recrystallization 17 mg (19%) of **RuT$_5$** and 20 mg (12%) of **RuT$_5$Ru**.

RuT$_5$. ^{1}H NMR (200 MHz, acetone-d_6): δ 9.19 (s, 2H), 9.11 (m, 2H), 8.74 (m, 11H), 8.10 (6H), 7.78 (m, 4H), 7.54 (m, 6H), 1.62 (m, 40H), 1.03 (m, 30H). UV−vis (CH_3CN) λ/nm (ϵ/M^{-1} cm^{-1}): 505 (56 300), 435 (63100), 308 (74 000), 272 (64 900). FAB$^+$ *m*/*z* (nature of the peak, relative intensity): 2059.3 ([M-PF$_6$]$^+$, 98), 2058.1 ([M-PF$_6$]$^+$, 100), 956.5 ([M-2PF$_6$]$^{2+}$, <5). Anal. Calcd for $C_{117}H_{121}N_9S_5RuP_2F_{12}$ (M_w = 2204.60): C, 63.74; H, 5.53; N, 5.72. Found: C, 63.57; H, 5.32; N, 5.34.

RuT$_5$Ru. ^{1}H NMR (200 MHz, acetone-d_6): δ 9.19 (s, 4H), 9.11 (d, J = 8.1 Hz, 4H), 8.87 (m, 8H), 8.62 (t, J = 8.1 Hz, 2H), 8.10 (m, 8H), 7.79 (m, 8H), 7.36 (m, 8H), thiophene alkyl chain protons are overlapping with residual solvent. UV−vis (CH_3CN) λ/nm (ϵ/M^{-1} cm^{-1}): 505 (81 500), 443 (68 300), 309 (112 900), 272 (94 100). FAB$^+$ *m*/*z* (nature of the peak, relative intensity): 2683.5 ([M-PF$_6$]$^+$, 100), 1269.3 ([M-2PF$_6$]$^{2+}$, 10). Anal. Calcd for $C_{132}H_{132}N_{12}S_5Ru_2P_4F_{24}\cdot CH_3OH$ (M_w = 2828.86 + 32.04): C, 55.84; H, 4.79; N 5.88. Found: C, 55.67; H, 4.78; N, 5.63.

Results and Discussion

Structures. The schematic structures of the ligands and complexes that are the focus of the present investigation are illustrated in Chart 1; for illustration purposes, an estimate of structural features for **RuT$_5$Ru** is shown in Chart 2. Preparation of the mono- and binuclear complexes was inspired by our previous syntheses of ruthenium(II) terpyridine complexes.[14,41] During these preparations, the ligands were allowed to react with *cis*-[Ru(terpy)(DMSO)Cl$_2$] after silver dehalogenation in a mixture of solvents under mild experimental conditions. Careful separation by chromatography and double recrystallization in adequate solvents allows isolation of the mononuclear and binuclear complexes in modest yields. These complexes were unambiguously characterized by proton NMR, FAB$^+$-MS, and elemental analysis as well as by cyclic voltammetry and UV−vis. The fingerprint of these complexes is shown by the aromatic part of the spectrum; for illustration purposes, Figure 1 compares proton NMR spectra for **RuT$_n$** and **RuT$_n$Ru**, n = 3 and 5. The number of aromatic patterns allows definitive assessment of the nature of the complex. The binuclear complex displays seven well-resolved patterns whereas in the less symmetric mononuclear complex, two additional and overlapping patterns at 8.75 and 7.50 ppm were observed. Integration of these aromatic patterns compared to the respective butyl protons of the thiophene fragments gives 42H for the binuclear complexes and 31H for the mononuclear species.

Electrochemistry. The electrochemical properties of the 5 ligands and 10 complexes were characterized by cyclic

(41) Benniston, A. C.; Grosshenny, V.; Harriman, A.; Ziessel, R. *Angew. Chem., Int. Ed. Engl.* **1994**, *33*, 1884.

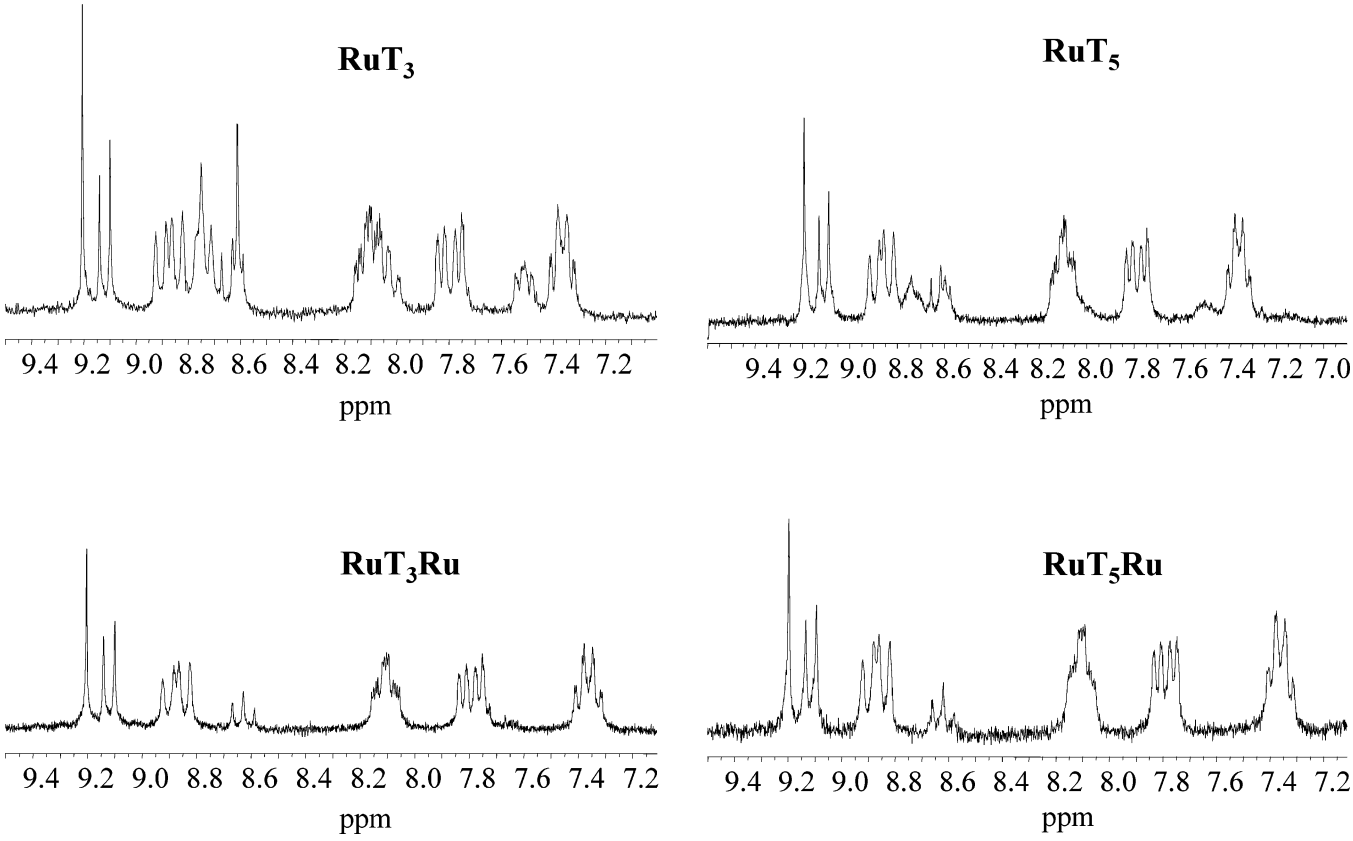

Figure 1. Proton NMR spectra (200 MHz) for **RuT*n*** and **RuT*n*Ru**, $n = 3$ and 5. For the sake of clarity, only the aromatic part of the complexes is represented.

Table 1. Electrochemical Properties of Ligands and Complexes[a]

compound	E_{ox}, V (ΔE_p)[b]	E_{red} (ΔE_p)[c]
T$_1$		
RuT$_1$	1.35 (60)	−1.14 (80); −1.38 (80)
RuT$_1$Ru	1.35 (80)	−1.16 (60); −1.41 (70)
T$_2$	1.32 (irr.)	
RuT$_2$	1.36 (60)	−1.14 (60); −1.36 (80)
RuT$_2$Ru	1.36 (80)	−1.15 (70); −1.41 (80)
T$_3$	1.33 (irr.)	
RuT$_3$	1.38 (60); 1.13 (irr.)	−1.14 (60); −1.39 (80); −1.65 (80)
RuT$_3$Ru	1.38 (80)	−1.13 (60); −1.38 (80)
T$_4$	1.21 (irr.)	
RuT$_4$	1.38 (60); 1.16 (irr.)	−1.14 (60); −1.34 (60); −1.66 (70)
RuT$_4$Ru	1.38 (80)	−1.13 (70); −1.32 (80
T$_5$	1.17 (irr.); 0.98 (irr.)	
RuT$_5$	1.39 (60); 1.11 (irr.)	−1.13 (80); −1.33 (80); −1.66 (100)
RuT$_5$Ru	1.39 (90)	−1.12 (80); −1.32 (80)
$[Ru(terpy)_2]^{2+}$	1.27 (60)	−1.27 (60); −1.51 (70)

[a] Potentials determined by cyclic voltammetry in 0.1 M $TBAPF_6/CH_3CN$ solution for the complexes and 0.1 M $TBAPF_6/CH_2Cl_2$ solution for the ligands (concentration 1.0×10^{-3} M for the complexes and 2.5×10^{-3} M for the ligands). Potentials were measured at a Pt working electrode referenced to a Pt wire quasi-reference electrode. Potentials were standardized using a ferrocene (Fc) internal reference and are converted to the SCE scale assuming that $E_{1/2}(Fc/Fc^+) = 0.38$ V. For the irreversible processes, the peak potential E_{AP} is quoted. [b] Metal- and thiophene-centered oxidations, see text. [c] Terpyridine-centered reductions, see text.

voltammetry in dichloromethane and CH_3CN solution, respectively. Table 1 lists the potentials (relative to the SCE reference electrode) for the waves that were observed in the +1.9- to −1.6-V potential range; data for the parent complex $[Ru(terpy)_2]^{2+}$ are also listed. A first observation is that for all of the ligands of the **T*n*** series there is no clear indication of either terpy- or thiophene-localized reduction within the given electrochemical window. However, although no oxidation signal is detected for **T$_1$**, an irreversible oxidation process is evidenced in the 1.32- to 0.98-V potential range for $n > 1$; in addition for the **T$_5$** ligand, two oxidation waves were observed. These results indicate that along the series oxidation at thiophene units is affected by the changes in electron density and charge delocalization occurring within the ethynyl-thiophene backbone.

All of the ruthenium complexes undergo a quasi-reversible oxidation process with half-wave potentials ($E_{1/2}^{ox}$) located in the 1.35−1.39-V range (Table 1). These metal-centered oxidation processes are more positive by at least 80 mV (by 120 mV for $n = 5$) compared to those of $[Ru(terpy)_2]^{2+}$, likely because of the electron-withdrawing character of the ethynyl-thiophene module.[22] For the binuclear complexes, a single wave is found for the Ru(II/III) couple, a fact that might indicate that the electronic coupling between the metal centers is relatively weak. For the mononuclear complexes with $n = 3$, 4, and 5, an additional irreversible oxidation wave located around 1.1 V was observed; this is likely to be ascribed to irreversible oxidation of the thiophene modules.[28,42] This oxidation step is not observed for the binuclear complexes.

All of the complexes exhibit two or three well-resolved reversible waves in the cathodic branch of the voltammograms. For each of the complexes, the first reduction is shifted to a more positive potential than that of the first

(42) Roncali, J. *J. Mater. Chem.* **1999**, *9*, 1875.

reduction of $[Ru(terpy)_2]^{2+}$ (data shown for comparison in Table 1), which is terpy-based.[10,14] This clearly indicates that in all of the new complexes the first reduction is localized on the coordinated terpy unit of the $\mathbf{T}_n$ ligand (owing to the electron-withdrawing character of the ethynyl-thiophene bridge). This first step is located at ca. −1.14 V for both the mononuclear and binuclear complexes. This corresponds to the addition of one electron for the mononuclear complexes, whereas for the binuclear ones, it was not clear if reduction was mono- or bielectronic (as expected in case the interposed ethynyl-thiophene decouples the terminal terpy units of the ditopic ligand); see Figure S1 of Supporting Information.

The addition of more electrons is likely to occur at the unsubstituted peripheral terpy ligand for both $\mathbf{RuT}_n$ and $\mathbf{RuT}_n\mathbf{Ru}$ complexes, consistent with the fact that the subsequent step observed is coincident for both cases (Table 1). In all cases, the second reduction is facilitated by at least 100 mV, whereas in some cases this difference reaches 190 mV compared to that of $[Ru(terpy)_2]^{2+}$ (Table 1), which also reflects the different electronic environment of these complexes. Interestingly, for the larger mononuclear complexes $\mathbf{RuT_3}$, $\mathbf{RuT_4}$, and $\mathbf{RuT_5}$, an additional wave is observed at a more cathodic potential, −1.65 V and is assigned to the reduction of the uncoordinated terminal terpy fragment of $\mathbf{T}_n$. This reduction takes place at a less negative potential than that of free terpy ($E_{1/2} = -1.89$ V),[43] which could be a consequence of the transmission of electron density to the 2+ metal center, which in turn helps the stabilization of the electrogenerated reduced species. This observation indicates that π overlap between the terpy and ethynyl-thiophene subunits actually occurs to some extent and that possible effects by the interposed ethynylthiophene modules do not completely decouple the terpy termini. Similar outcomes were reported in several recent studies of ruthenium complexes that feature bipyridine ligands bearing arylene-ethynylene,[44,45] oligomeric thiophene,[46] or thiophene-ethynylene substituents.[24]

Optical Spectroscopy. Absorption. Absorption and luminescence features for the investigated ditopic diethynyl-terpy ligands, $\mathbf{T}_n$ (Chart 1), have been reported.[38] Tables 2 and 3 list absorption and luminescence properties for the mononuclear $\mathbf{RuT}_n$ and binuclear $\mathbf{RuT}_n\mathbf{Ru}$ complexes. Figure 2 compares absorption profiles for the ligands and the mononuclear and binuclear complexes, parts a−c, respectively. An inspection of the Figure allows the identification of well-defined spectral portions. (See also absorption data collected in Tables 2 and 3.) These are examined below in some detail.

Transitions occurring in the UV region ($\lambda \leq 350$ nm, $\epsilon \approx 6-12 \times 10^4$ M^{-1} cm^{-1}) are ascribed to the ligand-localized nature, mainly of terpy origin, of both the free ligand (peaks at 285 nm, Figure 2, part a) and coordinated terpy fragments (peaks at 272 and 307 nm, parts b and c).

The bands in the 390- to 450-nm region (ϵ in the range of $(4-7) \times 10^4$ M^{-1} cm^{-1}) are ascribed to absorption by the oligomeric diethynyl-thiophene fragment of the ditopic ligands both as free (part a) and as bridging ligands (part b and c) as drawn by direct comparison of the absorption profiles in Figure 2. These bands are due to $\pi-\pi^*$ transitions occurring within the diethynyl-thiophene modules. Some intraligand CT character involving alkyl and thiophene units

Table 2. Photophysical Properties of $\mathbf{RuT}_n$ Mononuclear Complexes[a]

compound	λ_{max} (nm) ϵ_{max} (M^{-1} cm^{-1})	λ_{em} (nm)	$10^5 \times \phi_{em}$	τ (ns)[b]
$\mathbf{RuT_1}$	498 (43 800) 388 (43 200) 307 (71 600) 272 (67 100)	697 (703)	25.5	133
$\mathbf{RuT_2}$	503 (52 200) 422 (44 200) 307 (71 200) 273 (67 400)	718 (732)	5.2	158
$\mathbf{RuT_3}$	505 (56 100) 427 (56 500) 307 (73 100) 272 (67 300)	724 (760)	1.2	130
$\mathbf{RuT_4}$	505 (53 700) 433 (59 800) 307 (71 600) 272 (67 000)	716 (−)	0.9	110
$\mathbf{RuT_5}$	503 (56 300) 435 (63 100) 308 (74 000) 272 (64 900)	710 (−)	0.9	109

[a] In air-equilibrated acetonitrile solvent, room temperature, $\lambda_{exc} = 520$ nm; values in parentheses were obtained at 77 K. [b] Values obtained by monitoring the luminescence peak. Single exponentials were observed in each case.

Table 3. Photophysical Properties of $\mathbf{RuT}_n\mathbf{Ru}$ Binuclear Complexes[a]

compound	λ_{max} (nm) ϵ_{max} (M^{-1} cm^{-1})	λ_{em} (nm)	$10^5 \times \phi_{em}$	τ (ns)[b]
$\mathbf{RuT_1Ru}$	512 (79 700) 395 (40 100) 307 (117 400) 272 (90 600)	713 (708)	23.8	140
$\mathbf{RuT_2Ru}$	511 (92 300) 430 (46 900) 307 (116 900) 272 (90 800)	730 (735)	4.2	164
$\mathbf{RuT_3Ru}$	509 (100 200) 441 (58 100) 309 (116 000) 272 (91 400)	732 (760)	1.4	135
$\mathbf{RuT_4Ru}$	507 (107 800) 444 (72 100) 309 (115 900) 272 (93 500)	723 (765)	0.8	121
$\mathbf{RuT_5Ru}$	505 (81 500) 443 (68 300) 309 (112 900) 272 (94 100)	703 (−)	1.8	99

[a] In acetonitrile solvent, at room temperature, $\lambda_{exc} = 520$ nm. Values in parentheses were obtained at 77 K. [b] Values obtained by monitoring the luminescence peak. Single exponentials were observed in each case.

(43) Measured in dimethyl formamide at 80 °C using a hanging mercury electrode. Grosshenny, V. Thèse de l'Université Louis Pasteur, Strasbourg, 1996.
(44) Wang, Y. S.; Liu, S. X.; Pinto, M. R.; Dattelbaum, D. M.; Schoonover, J. R.; Schanze, K. S. *J. Phys. Chem. A* **2001**, *105*, 11118.
(45) Zhu, S. S.; Kingsborough, R. P.; Swager, T. M. *J. Mater. Chem.* **1999**, *9*, 2123.
(46) Trouillet, L.; De Nicola, A.; Guillerez, S. *Chem. Mater.* **2000**, *12*, 1611.

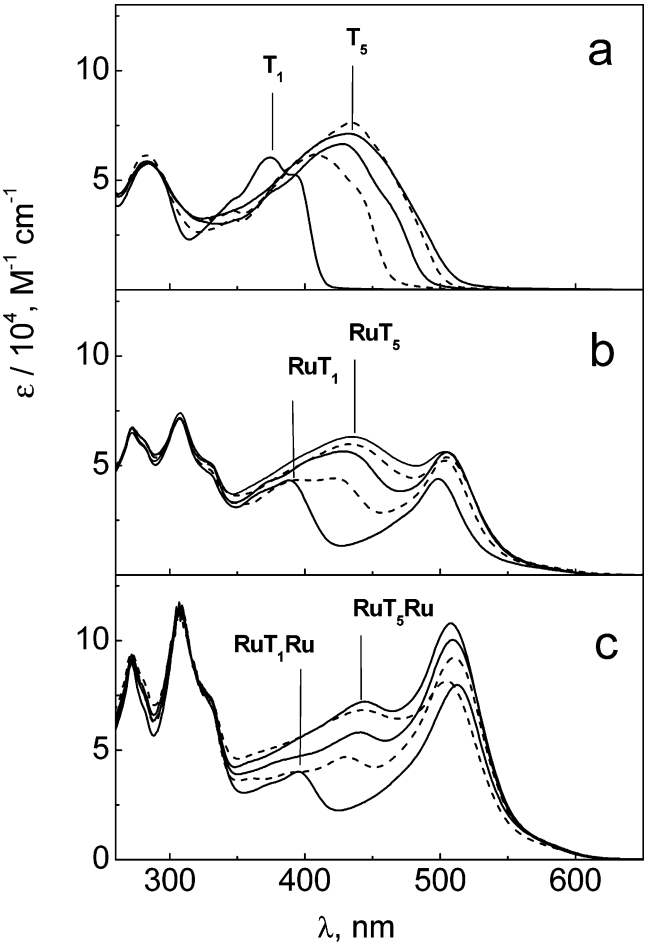

Figure 2. Ground-state absorption spectra for the series of five ligands (part a, in dichloromethane) and five mononuclear and five binuclear complexes (parts b and c, respectively, in acetonitrile). Only the first and last members of each series are labeled, $n = 1$ and 5, respectively.

as donors and terpys and acetylenic fragments as acceptors can also be present.[38] It is worth noticing that the peak maximum in this region undergoes a regular shift from 390 to 450 nm on going from one to five repeat diethynyl-thiophene units; a concomitant increase of the intensity of the band is also observed. This behavior indicates that the oligomeric diethynyl-thiophene linkage undergoes an effective electronic delocalization. However, the shift of the band maximum to lower energy on going from $n = 1$ to 5 reaches a plateau for $n \geq 3$, indicative of a saturation effect in the effective conjugation length, as previously noted.[38] Also worthy of note is that the position of the band maxima in the 390−450-nm region is identical, apart from the case of $n = 1$, for the free-ligand series and for the corresponding members (with the same n) of the series of the complexes (i.e., both for the dicationic $\mathbf{RuT}_n$ complexes and the tetracationic $\mathbf{RuT}_n\mathbf{Ru}$ complexes), Figure 2. The fact that the same extent of the shift is found for the series of the free ligand and of the corresponding mononuclear and binuclear complexes indicates that within the bridging ligands there is only a weak electronic connection between the oligomeric ethynyl-thiophene linkage as a whole and the terpy fragments (apart from the case of $n = 1$). This is consistent with the electrochemical behavior discussed above and with the small changes exhibited by the position of the metal-to-ligand charge-transfer (^{1}MLCT) absorption bands for both the mononuclear and binuclear complexes; see below.

For the absorption spectra of both the mononuclear and binuclear complexes (Figure 2, parts b and c, Tables 2 and 3), the spectral portion from 480 to 600 nm is ascribed to ^{1}MLCT transitions.[10,14] The position of the absorption maximum sticks very close to 505 nm in all cases, with the intensity of the ^{1}MLCT band for the complexes of the mononuclear series ($\epsilon \approx 5 \times 10^4$ M^{-1} cm^{-1}) being about half that of the corresponding complexes of the binuclear series. It can be noticed that the ^{1}MLCT transition for the parent $[Ru(terpy)_2]^{2+}$ complex, peaking at 490 nm, features a weaker transition intensity, $\epsilon = 1.7 \times 10^4$ M^{-1} cm^{-1}.[10] In comparison to this complex, the more intense ^{1}MLCT transition for the $\mathbf{RuT}_n$ series is likely due to a more extended delocalization at the coordinated fragments of $\mathbf{T}_n$. Similar cases where terpy-phenylene ligands were employed have been studied in detail[47] and provide hints on the correlation between MLCT band intensity and effects due to appended groups.[48] However, the fact that the ^{1}MLCT transition for the $\mathbf{RuT}_n\mathbf{Ru}$ series is twice as intense as that of the $\mathbf{RuT}_n$ series seems consistent with the somewhat localized nature of the transition, likely restricted to the proximate terpy-ethynyl fragment of $\mathbf{T}_n$.[14,22] That a localized approach well describes the nature of these transitions is further suggested by the fact that the peak for the CT band undergoes very small changes on going from the smallest ($n = 1$) to the largest size ($n = 5$) cases for both mononuclear and binuclear series; see Tables 2 and 3 and Figure 2. Furthermore, only a slight intensity increase (<20%) is observed along the two series (Figure 2), despite the presence of the underlying absorption tail of the oligomeric ethynyl-thiophene fragments (Figure 2, part a). In conclusion, the absorption results indicate that for both the uncoordinated and coordinated $\mathbf{T}_n$ ligands the oligomeric diethynyl-thiophene fragments as a whole undergo efficient delocalization but the metal-to-ligand interations within the complexes are somewhat confined to ligand portions close to the metal center.

Emission and Photophysics. Luminescence results obtained at room temperature and at 77 K are collected in Tables 2 ($\mathbf{RuT}_n$ mononuclear series) and 3 ($\mathbf{RuT}_n\mathbf{Ru}$ binuclear series), $n = 1$ to 5. Room-temperature luminescence spectra obtained by employing the indicated excitation wavelength are depicted in Figure 3. Regarding the $\mathbf{T}_n$ ligands, the interaction of $^1\pi-\pi^*$ and ^{1}CT states has been previously called for while discussing their fluorescence properties;[38] the possible effects related to the presence of rotamers were also examined in connection with the resolved profile of the fluorescence spectra as affected by the polarity of the solvent. For these ligands, the room-temperature band maximum is found to undergo a marked bathochromic shift

(47) Hammarström, L.; Barigelletti, F.; Flamigni, L.; Indelli, M. T.; Armaroli, N.; Calogero, G.; Guardigli, M.; Sour, A.; Collin, J. P.; Sauvage, J. P. *J. Phys. Chem. A* **1997**, *101*, 9061.
(48) Maestri, M.; Armaroli, N.; Balzani, V.; Constable, E. C.; Thompson, A. *Inorg. Chem.* **1995**, *34*, 2759.

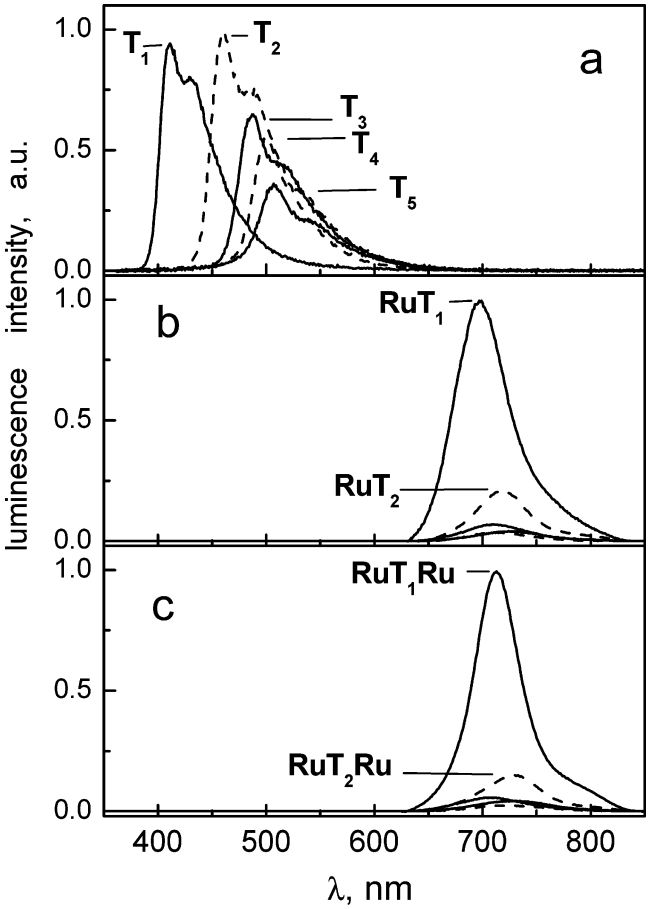

Figure 3. Room-temperature luminescence spectra for the $\mathbf{T}_n$ (dichloromethane, isoabsorbing solutions excited at $\lambda_{exc} = 340$ nm), and $\mathbf{RuT}_n$, and $\mathbf{RuT}_n\mathbf{Ru}$ series (acetonitrile, isoabsorbing solutions excited at $\lambda_{exc} = 520$ nm).

along with size (from $n = 1$ to 5).[38] This is shown in Figure 3, part a. Here it is also shown that the luminescence intensity decreases in the series (from $\phi = 0.18$ to 0.07 for $n = 1$ and 5, respectively, $\lambda_{exc} = 340$ nm). The room-temperature lifetimes for the $\mathbf{T}_n$ ligands are all $\tau < 1$ ns, consistent with the fluorescence nature of the emission. Regarding the $\mathbf{RuT}_n$ and $\mathbf{RuT}_n\mathbf{Ru}$ complexes, on the basis of their unresolved emission profiles (Figure 3), the luminescence lifetime range (~100 ns, Tables 2 and 3), and quantum yields ($\phi = 10^{-4}-10^{-5}$), the emission is ascribed to ^{3}MLCT states of predominantly Ru → terpy nature, as suggested by comparison with literature results.[10,14,22,49,50] The fact that for $n = 1$, for both the mononuclear and binuclear cases, a more intense (and long-lived) luminescence is observed than for the cases $n \geq 2$ may be explained in different ways, as discussed in points A, B, and C below.

A. A sizable electronic interaction between the terpy termini of the bridging ligands (and the metal centers for the cases of $\mathbf{RuT}_n\mathbf{Ru}$) could be allowed when these are not too far each other. This might be the case for $n = 1$, leading to "electronic delocalization" effects involving the terpy fragments, as reported in the literature.[19,20] On the contrary for $n \geq 2$, the lining up of several diethynyl-thiophene units could result in a weakening of the electronic interaction between the terpy termini.

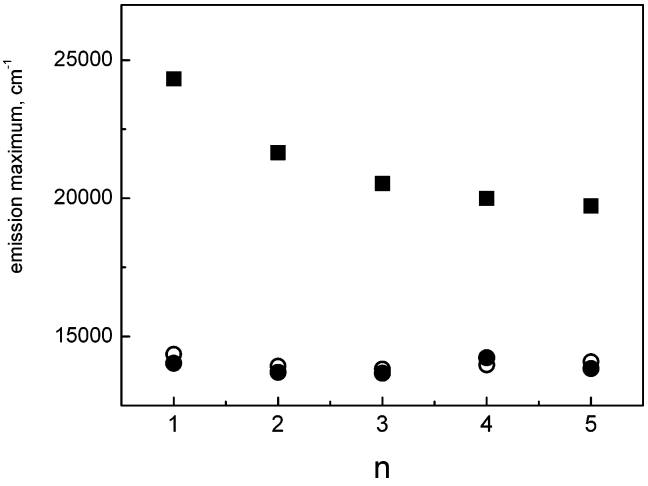

Figure 4. Changes of the band maxima for the ligand florescence (■) and the luminescence of the $\mathbf{RuT}_n$ mononuclear (○) and $\mathbf{RuT}_n\mathbf{Ru}$ binuclear (●) complexes in the series $n = 1$ to 5.

B. Another explanation could be based on the interplay of close-lying excited levels. For the Ru−polypyridine complexes, it is well known that the deactivation of the luminescent ^{3}MLCT levels to the ground level (GS) takes place via direct and mediated paths.[10,14] The direct path is governed by the "energy gap law" that states that rates for nonradiative paths are related to the energy of the emitting level.[51,52] The indirect path operates via thermal population of levels lying higher in energy than the emitting ^{3}MLCT level.[9,10,53] When these higher-lying levels are ^{3}MC in nature, enhanced nonradiative deactivation occurs owing to the strong MC−GS coupling. It is interesting that for both series of the mononuclear and binuclear complexes at room temperature the emission level seems scarcely affected by the size of the bridging ligand, Figure 3 (for results at 77 K, see below). This is likely to rule out any energy gap law effect for the diminished luminescence features for the complexes with $n \geq 2$.

C. Finally, an explanation for the luminescence behavior of Figure 3 could involve a role for the triplet level localized at the oligomeric diethynyl-thiophene fragments. The point is illustrated by Figure 4 where the change in the fluorescence maximum for the $\mathbf{T}_n$ ligands is compared with that for the luminescence of $\mathbf{RuT}_n$ and $\mathbf{RuT}_n\mathbf{Ru}$ complexes. It is noticed that for the $\mathbf{T}_n$ series, on going from $n = 1$ to 5, (i) the fluorescence level is stabilized by ca. 4500 cm^{-1} while the energy level of the emission for both $\mathbf{RuT}_n$ and $\mathbf{RuT}_n\mathbf{Ru}$ series undergoes smaller changes (see below for further data from 77 K results) and (ii) the fluorescence intensity becomes smaller and smaller (see Figure 3), which could be because of more effective intersystem crossing steps, leading to population of very weakly emitting (and elusive) triplet states

(49) Constable, E. C.; Housecroft, C. E.; Schofield, E. R.; Encinas, S.; Armaroli, N.; Barigelletti, F.; Flamigni, L.; Figgemeier, E.; Vos, J. G. *Chem. Commun.* **1999**, 869.
(50) Benniston, A. C.; Harriman, A.; Lawrie, D. J.; Mayeux, A. *Phys. Chem. Chem. Phys.* **2004**, *6*, 51.
(51) Englman, R.; Jortner, J. *Mol. Phys.* **1970**, *18*, 145.
(52) Kober, E. M.; Caspar, J. V.; Lumpkin, R. S.; Meyer, T. J. *J. Phys. Chem.* **1986**, *90*, 3722.
(53) Amini, A.; Harriman, A.; Mayeux, A. *Phys. Chem. Chem. Phys.* **2004**, *6*, 1157.

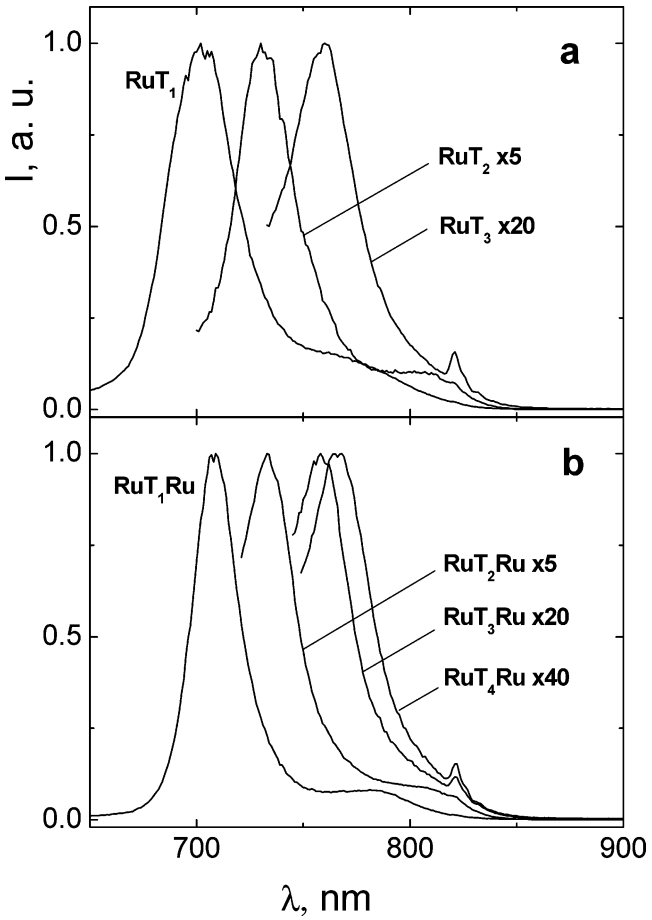

Figure 5. Normalized 77 K luminescence spectra for the indicated complexes, λ_{exc} = 520 nm. The magnification factors are approximate numbers.

centered on the diethynyl-thiophene fragments.[54] A direct assessment of the triplet energy level for the series $\mathbf{T}_n$ is not available; however, a plausible singlet−triplet energy separation is $\Delta E^{ST} \approx 5000$ cm^{-1}.[24,54] On this basis, on going from $n = 1$ to 5 it might be that the triplet energy level centered on the thiophene-ethynyl fragments, ^{3}LC($\mathbf{T}_n$), becomes closer and closer in energy to the ^{3}MLCT luminescence level(s), localized at the metal centers of $\mathbf{RuT}_n$ and $\mathbf{RuT}_n\mathbf{Ru}$ complexes, Figure 4. Thus, for the complexes, a ^{3}MLCT → ^{3}LC($\mathbf{T}_n$) deactivation path could become progressively available for increasing n values, resulting in depressed luminescence properties, as actually observed.

Luminescence results obtained at 77 K in frozen acetonitrile, for the complexes $\mathbf{RuT}_n$ (n = 1 to 3; no emission was detected for $n > 3$, Table 2) and $\mathbf{RuT}_n\mathbf{Ru}$ (n = 1 to 4; no emission was detected for $n = 5$, Table 3) are illustrated in Figure 5. From these results, one draws useful hints, as commented on below. (i) A first observation regards the fact that the luminescence peaks at 77 K are slightly bathochromically shifted with respect to what happens at room temperature. This behavior is opposite to that exhibited by most luminophores of the vast family of the Ru(II)−polypyridine complexes.[9,10] For these compounds, the formation of MLCT excited states results in substantial intramolecular charge redistribution. This is accompanied by the reorientation of solvent molecules (an effect related to the polarity of the solvent), and in fluid solvent, the ^{3}MLCT luminescence energy levels undergo some stabilization. In frozen solvent (as obtained at 77 K), such a stabilization effect cannot take place (the solvent molecules cannot reorient), and ^{3}MLCT luminescence spectra usually exhibit a hypsochromic shift with respect to what happens in fluid solvent. For the $\mathbf{RuT}_n$ (n = 1 to 3) and $\mathbf{RuT}_n\mathbf{Ru}$ (n = 1 to 4) complexes, the luminescence spectral profiles at 77 K (Figure 5) are consistent with a ^{3}MLCT nature for emission, as also found at room temperature. However, the 77 K luminescence intensity is very weak, and the observed behavior is probably related to the depletion of the ^{3}MLCT luminescence levels by lower-lying dissipative levels centered on the thiophene-based fragments (see below). (ii) On passing from $n = 1$ to higher numbers of repeat diethynyl-thiophene units, the ^{3}MLCT luminescence level undergoes a stabilization of ca. 1000 cm^{-1}, both for the mononuclear and binuclear complexes. This indicates that the ^{3}MLCT Ru → terpy levels are affected to some degree by delocalization occurring at the oligomeric fragments. (iii) On going from $n = 1$ to higher values, the luminescence intensity drops dramatically, which is similar to what happens at room temperature; see Figure 3. This latter observation excludes thermal activation to a higher-lying dissipative level as a cause for the observed luminescence quenching of the ^{3}MLCT luminescence levels along the series (Figure 5); instead it is consistent with the presence of lower-lying dissipative levels. These are likely to be the elusive triplet levels from the repeat thiophene-based fragments,[35] expected to become progressively stabilized for increasing n values; see Figure 3, part a. These triplet levels from the diethynyl-thiophene bridge would therefore be responsible for the observed vanishing of the ^{3}MLCT luminescence intensity in the larger mono- and binuclear complexes.

Regarding possible photoinduced electron-transfer processes within the complexes investigated, neither oxidative nor reductive steps, *Ru(II) → $\mathbf{T}_n$ and *Ru(II) ← $\mathbf{T}_n$ respectively, are allowed. Actually, at best the energy content of the ^{3}Ru−terpy level is estimated to be ≤1.8 eV (corresponding to $\lambda_{em}^{max} \approx 700$ nm at 77 K, see Tables 2 and 3), and on the basis of the electrochemical results of Table 1, the driving force is always unfavorable by at least 0.4 eV.

As a final point, we note that the complexes exhibit slightly enhanced luminescence properties in oxygen-free (de) solvent at room temperature. For instance, for $\mathbf{RuT}_1$, $\phi^{de} = 4.8 \times 10^{-4}$ and $\tau^{de} = 240$ ns, which represents a doubling factor with respect to what happens for the air-equilibrated case; see Table 2. Likewise, for $\mathbf{RuT}_1\mathbf{Ru}$, $\phi^{de} = 8.6 \times 10^{-4}$ and $\tau^{de} = 560$ ns, 4 times the values found for the air-equilibrated case, Table 3. Given that for air-equilibrated acetonitrile [O_2] $= 1.9 \times 10^{-3}$,[55] eq 2 provides estimates for the rate constant of diffusional quenching by dioxygen, k_q.[56]

$$\frac{\tau^{de}}{\tau} = \frac{\phi^{de}}{\phi} = 1 + k_q \tau^{de}[O_2] \qquad (2)$$

(54) Rothe, C.; Hintschich, S.; Monkman, A. P.; Svensson, M.; Anderson, M. R. *J. Chem. Phys.* **2002**, *116*, 10503.

Accordingly, we found k_q to be 1.8×10^9 and 2.8×10^9 M^{-1} s^{-1} for **RuT$_1$** and **RuT$_1$Ru**, respectively, to be compared with 2×10^9 M^{-1} s^{-1} for $[Ru(bpy)_3]^{2+}$.[57,58] The smaller value of k_q for the mononuclear complex could be due to a sort of shielding effect by the pendant **T$_1$** ligand toward the portion of the **RuT$_1$** molecule actually bearing the Ru → terpy excitation; statistical reasons might also be involved. (For **RuT$_1$Ru**, there are two centers for bearing the excitation, even if not simultaneously available.) However, the issue of possible differences toward oxygen quenching effects between the mononuclear and binuclear complexes was not systematically investigated because of the small luminescence intensities observed for $n > 1$ (Tables 2 and 3).

Conclusions

The synthesis and characterization together with the electrochemical and photophysical properties of a new series of wirelike Ru-terpyridine complexes are reported. The complexes contain ethynyl-linked, 3,4-dibutylthiophene-substituted terpyridine ligands so that their length ranges from 2 to 4 nm for a number of the ethynyl-thiophene modules varying from 1 to 5. For all cases, the oxidation of the ruthenium center(s) occurs in the same potential range, without any significant splitting of the waves for the binuclear complexes. In the mononuclear complexes, an additional, irreversible thiophene-based oxidation is observed with the higher number of ethynyl-thiophene modules. Well-resolved reduction potentials are found, corresponding to reduction steps at the various terpy segments. The absorption spectra of the complexes feature several types of transitions, either localized on the ligands (both on terpy and ethynyl-thiophene subunits) or of MLCT (Ru → terpy) nature. The high intensity of the transitions in the visible region (ϵ in the range of $(4-10) \times 10^4$ M^{-1} cm^{-1}) can prove useful in view of relevant applications.[1−8] The photophysical properties of the complexes are apparently dominated by relatively long-lived ^{3}MLCT luminescent excited states ($\tau = 100-160$ ns, at room temperature), which are ascribed to largely localized Ru → terpy character. For both the **RuT$_n$** and **RuT$_n$Ru** series, the electrochemical and spectroscopic results indicate that the electronic interaction between the terpyridine subunits of the **T$_n$** ligands (as mediated by the interposed diethynyl-thiophene oligomeric fragments) is weak, particularly for the larger molecules, $n \geq 3$. The weak coupling between terpy and diethynyl-thiophene subunits could explain why low-lying $^3\pi-\pi^*$ triplet states localized at the oligo ethynyl-thiophene framework do not completely quench the ^{3}MLCT luminescence. However, photoinduced intramolecular electron transfer (both for oxidative or reductive schemes), as driven by the energy content of the excited Ru-terpy levels and involving the diethynyl-thiophene fragments, is inhibited by an unfavorable energetic balance in all cases. Given the interest of such wirelike complexes as molecular components of thiophene-based photonic devices and to gain control over competitive energy disposal paths, we are currently using ligand tailoring to adjust the energy levels of the excited states localized at the Ru-based and thiophene-based portions of the species.

Acknowledgment. The FIRB project RBNE019H9K "Molecular Manipulation for Nanometric Devices" by MIUR and the Centre national de la Recherche Scientifique are acknowledged for financial support. Céline Rigenbach is acknowledged for the preparation and purification of the ligands. We are grateful to Dr. Abderrahim Khatyr for preliminary electrochemical measurements.

Supporting Information Available: Figure showing the cyclic voltammograms of the mononuclear **RuT$_3$** and the dinuclear **RuT$_3$Ru** complexes. This material is available free of charge via the Internet at http://pubs.acs.org.

IC0493043

(55) Murov, S. L.; Carmichael, I.; Hug, G. L. *Handbook of Photochemistry*; Marcel Dekker: New York, 1993.
(56) Lakowicz, J. R. *Principles of Fluorescence Spectroscopy*; Plenum: New York, 1999.
(57) Demas, J. N.; Harris, E. W.; McBride, R. P. *J. Am. Chem. Soc.* **1977**, *99*, 3547.
(58) Abdel-Shafi, A. A.; Beer, P. D.; Mortimer, R. J.; Wilkinson, F. *Helv. Chim. Acta* **2001**, *84*, 2784.